

COMPUTATIONAL PREDICTION OF PENETRATION SHAPES IN MIG WELDING OF PRACTICAL ALUMINUM ALLOY JOINTS

H. SERIZAWA*, S. SATO** and F. MIYASAKA**

**Joining and Welding Research Institute, Osaka University*

***Graduate School of Engineering, Osaka University*

DOI 10.3217/978-3-85125-615-4-02

ABSTRACT

As one of the methods for simulating the molten droplet from filler wire in metal insert gas (MIG) welding, a new line-type heat source has been developed and it is added in the three-dimensional, non-stationary thermal model which can demonstrate both molten pool and penetration shape in gas metal arc welding (GMAW) process. As the result of the examination about the applicability of this combined model for the practical aluminum joint, it is found that the penetration shape in the lap joint can be fairly demonstrated by assuming the adiabatic condition due to the oxide layer and/or the physical separation. In addition, it is revealed that the overhang length of numerical joggle joint model should be appropriately shortened in order to reproduce the penetration shape of practical joggle joint. Moreover, it can be concluded that the penetration shape of the practical aluminum joints can be reproduced by defining the dominant parameters in the combined model through the examinations of the basic welding.

INTRODUCTION

Recently, the aluminum alloys have been widely employed in the transportation equipment, such as railway vehicle, car vehicle, motor bicycle and so on, in order to reduce the total weight of equipment and/or to decrease the carbon dioxide emission [1-3]. Although the friction stir welding (FSW) has been positively used for joining the aluminum alloy due to its various advantages such as less decrement of mechanical strength, small distortion after joining and so on [4,5], the thickness of plates is generally limited to be less than 10 mm and it is difficult to join the complicate shape structures by using FSW. Then, the metal insert gas (MIG) welding has been generally employed for joining the aluminum alloy parts in the motor bicycle [3], where the penetration shape becomes the finger type [6,7].

As for the methods to simulate gas metal arc welding (GMAW) process, many attempts have been made [8-10]. Dilthey and Roosen have studied a three-dimensional, quasi-stationary thermal model for GMAW [8]. In the model, the influence of process parameters such as the wire diameter and the composition of the shielding gas on the weld profile can be taken into account. Kim and Na have proposed a model of GMAW including the effect of weld pool convection [9]. Pardo and Weckman have developed a model for the

Mathematical Modelling of Weld Phenomena 12

prediction of weld pool and reinforcement dimensions in GMAW welds using a finite element method, which has been formulated for a moving coordinate framework [10]. In spite of these efforts, some problems remain to be solved because of the complexity of arc welding processes. For example, the models mentioned above are for quasi-stationary conditions. In GMAW process, the electrode wire is melted and supplied to the molten pool intermittently and the welding process is fairly dynamic.

On the other hand, in order to examine the dynamic behaviour of weld pool precisely, Cao, Yang and Chen have developed a three-dimensional transient thermos-fluid model with free surface which can simulate the interaction of a metal droplet with the weld pool and shows a good agreement between the predicted finger penetration and actual welds [11]. Kumar and DebRoy have combined a heat transfer model with an optimization algorithm to determine several uncertain welding parameters from a limited volume of experimental data and the finger penetration characteristic of GMAW welds computed was in fair agreement with the experimental results for various welding conditions [12]. However, these models include many parameters which should be estimated through various computations or inverse analyses, and the typical features of GMAW process such as undercutting and humping cannot be reproduced.

As one of the methods for simulating GMAW process simply and practically, Yamamoto, Ohji, Miyasaka and Tsuji have developed a three-dimensional, non-stationary thermal model [13]. By using a finite difference model based on the heat flow equation and taking account of the balance of gravity, surface tension and arc pressure, both the molten pool and the penetration shape in the various types of GMAW are successively demonstrated [13-15]. In addition, by developing a new line-type heat source, which models the molten droplet from filler wire, and combining this line-type heat source with the three-dimensional, non-stationary thermal model, the penetration shapes in bead-on MIG welding and butt MIG welding with V-groove have been successfully reproduced [16]. In this research, in order to examine the applicability of this combined model for the practical aluminum joints, the penetration shapes in lap and joggled joints were studied.

METHOD FOR ANALYSIS

MODEL FOR GMAW PROCESS

In order to simplify the numerical model for GMAW process, the following two assumptions have been employed.

- The heat flow in the weld pool is assumed to be conductive. Namely, the influence of the metal flow in the weld pool is neglected.
- The weld pool is set to be in a static equilibrium under the influence of gravity, surface tension and arc pressure.

Based on the above two assumptions, the governing equations are as follows,

$$\rho \frac{\partial H}{\partial t} = \frac{\partial}{\partial x} \left(K \frac{\partial T}{\partial x} \right) + \frac{\partial}{\partial y} \left(K \frac{\partial T}{\partial y} \right) + \frac{\partial}{\partial z} \left(K \frac{\partial T}{\partial z} \right) \quad (1)$$

Mathematical Modelling of Weld Phenomena 12

$$\sigma \left[\frac{(1 + \xi_y^2) \xi_{xx} + (1 + \xi_x^2) \xi_{yy} - 2 \xi_x \xi_y \xi_{xy}}{(1 + \xi_x^2 + \xi_y^2)^{3/2}} \right] = \rho g \xi + P_a - \lambda \quad (2)$$

Where, ρ , H , K , and T in Eqn. (1) are density, enthalpy, thermal conductivity and temperature, respectively. σ , ξ , g , P_a and λ in Eqn. (2) are surface tension, surface displacement, gravity acceleration, arc pressure and Lagrange multiplier, respectively. Equation (1) is used for estimating the temperature distribution in the base metal, while the theoretical configuration of the molten pool in the model is derived from Eqn. (2). Figure 1 shows the schematic illustration of the calculation flow during a unit time step in this model. The torch is fixed during the time step (Fig. 1(i)) and the thermal energy is transferred into the base metal from the arc (Fig. 1(ii)). In the final stage of this unit time step, the amount of the wire melted during this time step is transferred on the molten pool (Fig. 1(iii)) and the surface profile is calculated using Eqn. (2) (Fig. 1(iv)). Once the calculation for the unit time step is completed, the torch is moved and the calculation for the next time step is repeated in a similar manner.

As a numerical method for modelling GMAW process, three-dimensional finite difference method was employed. So, the grid points for both the target material and the air space surrounding the target material are configured in the numerical space as shown in Fig. 2, and the variables are set to each grid points.

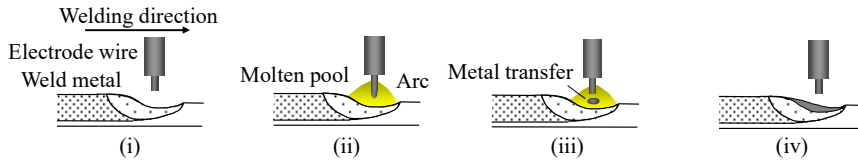


Fig. 1 Process of GMAW.

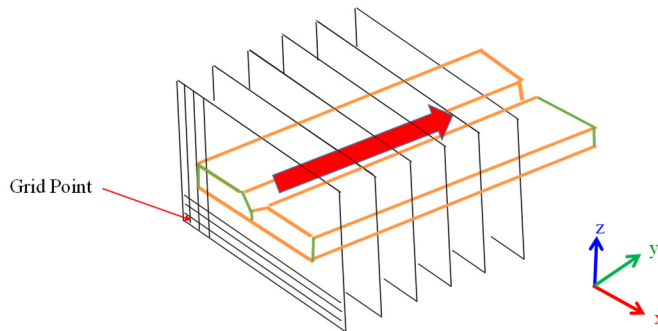


Fig. 2 Schematic illustration of numerical space in finite difference method.

LINE-TYPE HEAT SOURCE

Mathematical Modelling of Weld Phenomena 12

In the above model, the heat source is assumed to be distributed in a circular zone on the molten pool. However, because the finger type penetration in MIG welding is caused by the molten droplet from the filler wire to the bottom of the molten pool and the molten droplet would have a high speed and a high temperature [6], the internal heat source in the molten pool should be also taken into account. So, in this research, a new line-type heat source model has been developed and has been combined in the original model for GMAW process based on the following assumptions.

- The thermal energy is assumed to be divided into that from the arc and the molten droplet. Namely, the thermal energy from the arc is defined by the original heat source distributed on the molten pool, while that from the droplet is modeled by the line-type heat source.
- The line-type heat source is set to be uniformly distributed from the top surface to the bottom of the weld pool.

Then, the shape of line-type heat source changes as shown in Fig. 3. In the beginning of welding, the line-type heat source starts as a punctiform heat source at the center of the circular zone on the surface defined by the original heat source. With the growth of molten pool, the length of line-type heat source becomes longer. In this combined model, a ratio of the thermal energy from the original heat source to that from the line-type heat source is defined as a “ratio of heat source”.

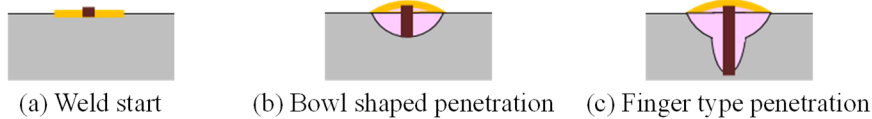
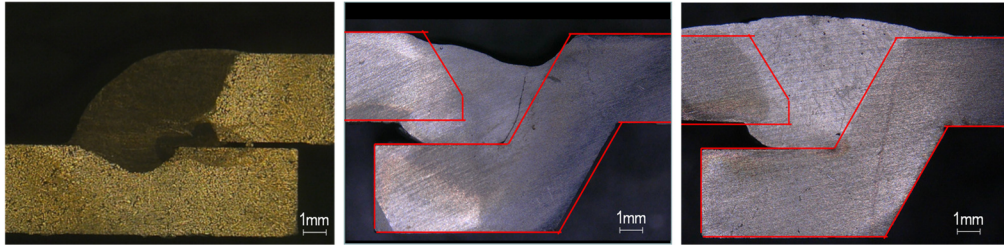


Fig. 3 Change of heat source shape.

OBJECTS FOR ANALYSIS

As the examples of practical aluminum joints, lap and joggled joints were examined in this research. The penetration shapes obtained in the experimental welding of lap and joggled joints are shown in Fig. 4, where forging and extruded aluminum alloys were employed as same as the practical joints, respectively. The thickness of aluminum alloys is 4 mm. The welding conditions of each joints are shown in Table 1. In addition, Fig. 5 is a schematic drawing of the joggle joint. Although two passes welding is employed for producing the practical joggle joint, both one pass and two passes welding were conducted in the experiment in order to examine the influence of welding pass on the penetration shape precisely, and both the penetrations are also shown in Fig. 4. In this research, in order to reproduce the penetrations shown in Fig. 4, the computational analyses using the combined model were conducted. In order to reduce the calculation time, the sizes of numerical models were set to be smaller than those of the experiments without affecting the penetration shape computed. Table 2 shows the model sizes and other parameters in the combined model.

Mathematical Modelling of Weld Phenomena 12



(a) Lap joint (b) Joggle joint (after 1st pass) (c) Joggle joint (after 2nd pass)

Fig. 4 Penetration shapes obtained in practical aluminum joints.

Table 1 Welding conditions for practical aluminum joints.

| | | Lap Joint | Joggle Joint |
|------------------------|----------------------------|------------------|---------------------|
| Size of plate | (mm) | 200 x 200 x 4 | 150 x 100 x 4 |
| Welding speed | (cm/min) | 72 | 72 |
| Current | (A) | 150 | 140 |
| Voltage | (V) | 20 | 20 |
| Weaving | Full amplitude (mm) | 4 | 4 |
| | Frequency (Hz) | 2.8 | 2.8 |
| Overlap space | (mm) | 5 | - |
| Gap width | (mm) | 0 | - |
| Target position | | Overlaid corner | Bottom corner |
| Torch angle | (degree) | 55 | 90 |
| Wire diameter | (mm) | 1.2 | 1.2 |

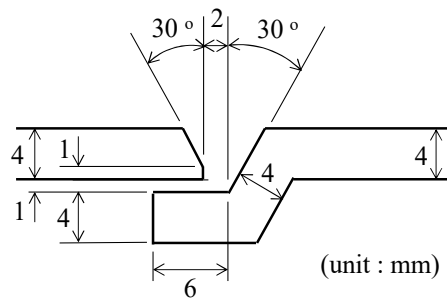


Fig. 5 Schematic drawing of joggle joint.

Table 2 Typical conditions for numerical analyses.

| | | Lap Joint | Joggle Joint |
|-------------------------------|------|------------------|---------------------|
| Size of plate | (mm) | 100 x 50 x 4 | 150 x 75 x 4 |
| Thermal efficiency | (%) | | 70 |
| Ratio of heat source | | | 7 : 3 |
| Radius of arc pressure | (mm) | 4 | 4 (1st pass) |
| | | | 5 (2nd pass) |

RESULTS AND DISCUSSIONS

LAP JOINT

According to the previous studies about the various GMAW processes using the three-dimensional, non-stationary thermal model and our research about bead-on MIG welding and butt MIG welding with V-groove using the combined model, it is revealed that the penetration shapes would be predicted regardless of the joint geometry by defining the dominant parameters in the model, which are dependent on the welding equipment [11]. In this research, the dominant parameters, which are thermal efficiency, ratio of heat source and radius of arc pressure, area assumed to be the values obtained from our previous research as shown in Table 2. The material properties were decided from our measurement for the aluminium alloy used in the experiment. The density, thermal conductivity, latent heat, specific heat and surface tension were set to be 2.78 Mg/m^3 , $170 \text{ W/(m}\cdot\text{K)}$, 333 kJ/kg , $1000 \text{ J/(kg}\cdot\text{K)}$ and 0.8 N/m , respectively. Figure 6 shows the maximum temperature distribution and the penetration shape of lap joint computed, and it is found that the surface profile of weldment has a very good agreement with the experiment, while the depth of penetration to the bottom plate which seems to affect the lap joint strength is shallower than the experimental result. One possible reason for this shallow penetration is considered to be the difference of thermal conductivity of two plates before the welding. The two plates are set to be joined thermally in this numerical model, while upper and bottom plates are not integrated thermally due to the oxide layer on the surface of aluminum alloy and/or small physical separation of two plates in the experiment. In the practical welding, thermal energy from arc and molten droplet seems to concentrate on the weld pool because the thermal conductivity between two plates would be prevented by the oxide layer and/or the physical separation, and then the depth of penetration to the bottom plate might become to be deeper.

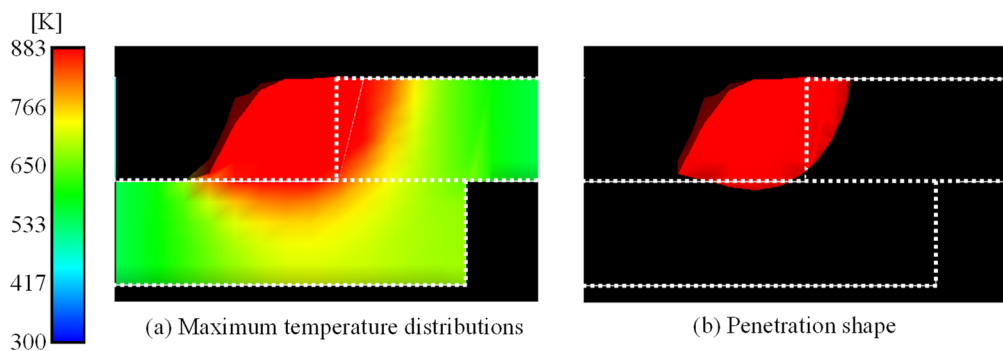


Fig. 6 Maximum temperature distribution and penetration shape of lap joint computed.

In order to overcome this difference, the two plates are assumed to be separated and be insulated thermally before generating the weld pool between two plates and the two plates change to be integrated after producing the weld pool. In other words, the adiabatic condition due to the oxide layer and/or the physical separation is set at the overlap space

Mathematical Modelling of Weld Phenomena 12

before welding. The penetration shape computed by using the modified model is shown in Fig. 7 and it is found that that its depth to the bottom plates seems to be slightly deeper than that of the original model shown in Fig. 6(b). Because there was a gap between the two plates obviously after welding as shown in Fig. 4(a), there would still be a difference of the thermal conductivity between the modified model and the experiment. In addition, the target position might be shift to the bottom plate although it is set to be the overlaid corner before welding. Although there still be a difference in the depth of penetration to the bottom plate between the numerical and experimental results, the modification of the model assuming the adiabatic condition before welding is considered to be effective for predicting the penetration shape of practical lap joint.

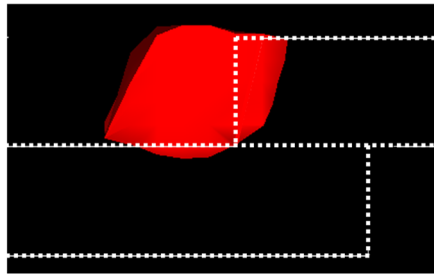


Fig. 7 Penetration shape of lap joint with assuming adiabatic condition before welding.

JOGGLE JOINT

According to the results of lap joint, the penetration shape is computed by assuming the adiabatic condition due to the oxide layer, and the results of maximum temperature distribution and penetration shape after first pass welding are shown in Fig. 8. From this figure, it is found that the depth of deposit metal calculated is shallower than that in the experiment. In addition, the filler metal fully flowed into the gap in the numerical result although only 2/3 of gap was filled in the experiment as shown in Fig. 4(b). In the practical process, the surface of filler metal in the gap would be slightly solidifying with flowing into the gap continuously. However, because the surface profile of filler metal flowed into the gap is only derived from Eqn. (2) and the flow process of filler metal is not modeled, the filler metal seems to achieve to the edge of gap in this computation.

In order to solve this problem, the amount of filler metal flowed is controlled by changing the overhang length of joggle joint. In this study, the overhang length which is 6 mm originally, is shortened to be 3 or 4 mm because about 2/3 of gap was filled in the experiment. Figure 9 shows the penetration shapes computed after first pass welding. In both cases, the filler metal fully flowed into the gap but it did not overflow. Then, the depth of deposit metal becomes deeper and the results show good agreements with the experiment. However, because the amount of filler metal flowed in the case of 3 mm overhang would be smaller than that in the experiment and the thermal energy would concentrate on the groove, the penetration would become to be larger than that in the case of 4 mm overhang. In order to examine the applicability of the combined model for the practical joggle joint, the penetration shape after second pass is also computed where the overhang length is assumed to be 3 or 4 mm as same as the cases for first pass. The results

are shown in Fig. 10 and it is revealed that the thermal energy applied in second pass would not almost affect the penetration produced in first pass and the filler metal deposited in the groove is mainly influenced by this second heat input. In addition, the numerical result of 4 mm overhang has a very good agreement with the experimental result after the second pass and it can be concluded that the penetration shape of the practical joggle joint can be reproduced by combined model with assuming the appropriate overhang length. Moreover, from our previous studies about the basic aluminum joints and these researches about the practical joints, it is found that the penetration shape of the practical aluminum joint can be reproduced by defining the dominant parameters in this combined model through the examinations of the basic welding such as bead-on welding, butt joint welding with the groove and so on.

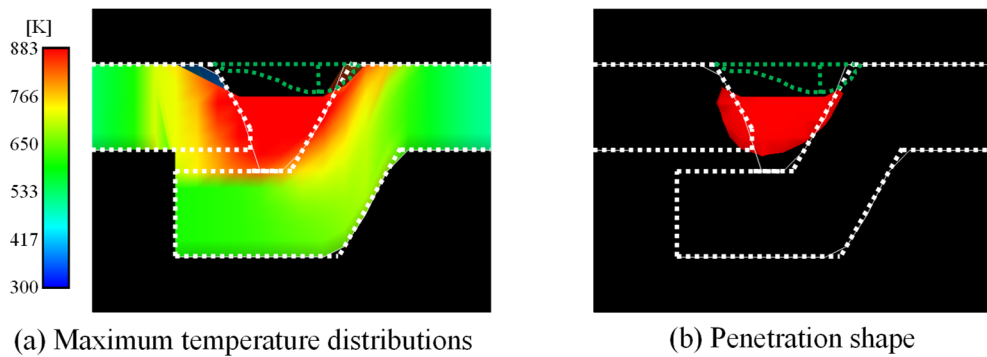


Fig. 8 Maximum temperature distribution and penetration shape of joggle joint after 1st pass.

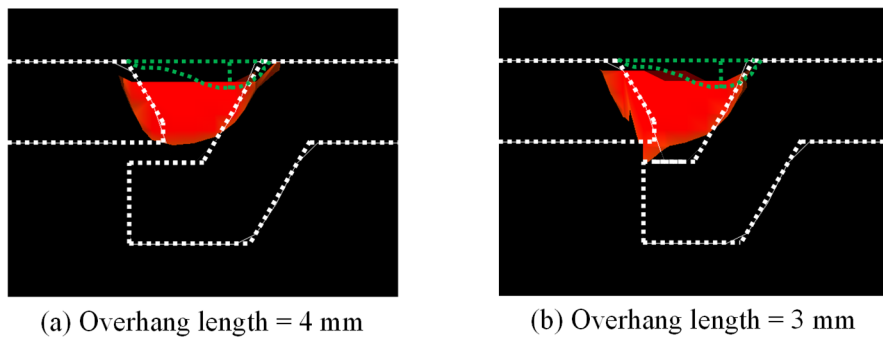


Fig. 9 Effect of overhang length on penetrations of joggle joint after 1st pass.

Mathematical Modelling of Weld Phenomena 12

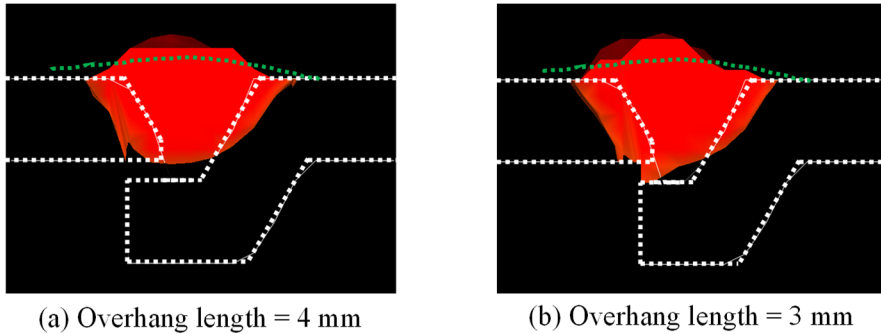


Fig. 10 Effect of overhang length on penetrations of joggle joint after 2nd pass.

CONCLUSIONS

In order to demonstrate the finger type penetration generated in MIG welding, a new line-type heat source has been combined with the three-dimensional, non-stationary thermal model and this combined model is applied for reproducing the practical aluminum lap and joggle joints. The conclusions can be summarized as follows,

- By assuming the adiabatic condition due to the oxide layer and/or the physical separation, the penetration shape in the lap joint can be fairly demonstrated, because the oxide layer on the aluminum alloy and/or the physical separation prevent the thermal conductivity.
- Because the combined model cannot simulate the flow process of filler metal and the filler metal achieves to the edge of gap regardless of overhang length in the joggle joint, the overhang length in the numerical model should be appropriately shortened in order to reproduce the penetration shape in the practical joggle joint.
- The penetration shape of the practical aluminum joints can be reproduced by defining the dominant parameters in the combined model through the examinations of the basic welding.

ACKNOWLEDGEMENTS

The authors would like to express their sincere appreciation to T. Mizuno and M. Enyama (Suzuki Motor Corporation) for providing the experimental data of penetration shapes in the MIG welding of aluminum alloy.

REFERENCES

- [1] U. DILTHEY AND L. STEIN: 'Technical Trends and Future Prospects of European Automotive Industry', *Proceedings of the 57th IIW International Conference on Technical Trends and Future Prospectives of Welding Technology for Transportation, Land, Sea, Air and Space*, pp. 19-30, 2004.

Mathematical Modelling of Weld Phenomena 12

- [2] H. NISHIKAWA AND M. FUJIMOTO: 'Control of Rotational Distortion in Friction Stir Welding', *Proceedings of the 57th IIW International Conference on Technical Trends and Future Prospectives of Welding Technology for Transportation, Land, Sea, Air and Space*, pp. 79-85, 2004.
- [3] H. SERIZAWA, T. YAMAMOTO, H. MURAKAWA, T. MIZUNO, M. ENYAMA AND F. MATSUDA: 'Prediction of Welding Distortion in a Part of Motorcycle Using Inherent Deformations Obtained from Inverse Analysis for Aluminum Alloy Welded Joints', *Trends in Welding Research, Proceedings of the 8th International Conference*, pp. 774-780, 2009.
- [4] H. SERIZAWA, J. SHIMAZAKI AND H. MURAKAWA: 'Numerical Study of Factors for Generating Inherent Strain in Friction Stir Welding', *Trends in Welding Research 2012, Proceedings of the 9th International Conference*, pp. 922-929, 2013.
- [5] U. SUHUDDIN, L. CAMPANELLI, M. BISSOLATTI, H. WANG, R. VERASTEGUI, J.F. DOS SANTOS: 'A Review on Microstructural and Mechanical Properties of Friction Spot Welds in Al-based Similar and Dissimilar Joints', *Proceedings of the 1st International Joint Symposium on Joining and Welding*, pp. 15-21, 2013.
- [6] W.G. ESSERS AND R. WALTER: 'Heat Transfer and Penetration Mechanisms with GMA and Plasma-GMA Welding', *Welding Research Supplement*, February, pp. 37-s-42-s, 1981.
- [7] M. SHOEB, M. PARVEZ AND P. KUMARI: 'Effect of MIG Welding Input Process Parameters on Weld Bead Geometry on HSLA Steel', *International Journal of Engineering Science and Technology*, Vol. 5, No. 1, pp. 201-212, 2013.
- [8] U. DILTHEY AND S. ROOSEN: 'Computer simulation of Thin sheet Gas-Metal-Arc-Welding'. *Proceedings of International Symposium on Theoretical Prediction in Joining and Welding*, Joining and Welding Research Institute, Osaka University, pp.133-154, 1996.
- [9] J.-W. Kim and S.-J. Na: 'A Study on the Three-Dimensional Analysis of Heat and Fluid Flow in Gas Metal Arc Welding Using Boundary-Fitted Coordinates', *Journal of Engineering for Industry*, Volume 116, Issue 1, pp.78-85, 1994.
- [10] E. PARDO AND D.C. WECKMAN: 'Prediction of Weld Pool and Reinforcement Dimensions of GMA Welds Using a Finite-Element Model', *Metallurgical Transactions B*, Vol. 20B, pp.937-947, 1989.
- [11] Z. CAO, Z. YANG AND X.L. CHEN: 'Three-Dimensional Simulation of Transient GMA Weld Pool with Free Surface', *Welding Journal*, June, pp.169-S-176-S, 2004.
- [12] A. KUMAR AND T. DEBROY: 'Guaranteed Fillet Weld Geometry from Heat Transfer Model and Multivariable Optimization', *International Journal of Heat and Mass Transfer*, Vol. 47, pp.5793-5806, 2004.
- [13] T. YAMAMOTO, T. OHJI, F. MIYASAKA AND Y. TSUJI: 'Mathematical Modelling of Metal Active Gas Arc Welding', *Science and Technology of Welding and Joining*, Vol. 7, No. 4, pp. 260-264, 2002.
- [14] T. YAMAMOTO, Y. YAMAZAKI, Y. TSUJI, F. MIYASAKA AND T. OHJI: 'Simulation Software of MAG Arc Welding for Butt Joint', *Quarterly Journal of the Japan Welding Society*, Vol. 23, No. 1, pp. 71-76, 2005 (in Japanese).
- [15] Y. YAMAZAKI, F. MIYASAKA AND T. OHJI: 'A Simulation Model for High Speed MAG Welding for Thin Plate', *Quarterly Journal of the Japan Welding Society*, Vol. 24, No. 4, pp. 368-372 2006 (in Japanese).
- [16] H. SERIZAWA, M. YOSHIYAMA AND F. MIYASAKA, 'Development of Line-type Heat Source for Finger Type Penetration in MIG Welding', *Mathematical Modelling of Weld Phenomena 11*, Verlag der Technischen Universität Graz, pp.51-61, 2017.